IOP Conf. Series: Journal of Physics: Conf. Series **876** (2017) 012021 doi:10.1088/1742-6596/876/1/012021

Oxygen-15+α resonant elastic scattering to study cluster states in ^{19}Ne

D Torresi[1], C. Wheldon[1], Tz. Kokalova[1], S. Bailey[1], A. Boiano[2], C. Boiano[3], M. Cavallaro[4], S. Cherubini[4], A. Di Pietro[4], J.P. Fernandez Garcia[4], M. Fisichella[4], T.R. Glodariu[5], J. Grebosz[6], M. La Cognata[4], M. La Commara[2,7], M. Lattuada[4,8], M. Mazzocco[9,10], D. Mengoni[9,10], C. Parascandolo[2,7], D. Pierroutsakou[4], G. Pizzone[4,8], C. Signorini[10], C. Stefanini[9], L. Stroe[5], C. Spitaleri[4,8], E. Strano[9,10], and M. Zadro[11]

[1]School of Physics and Astronomy, University of Birmingham, Birmingham, B15 2TT, UK
[2]INFN-Sezione di Napoli, Via Cinthia, I-80126 Napoli, Italy
[3]INFN-Sezione di Milano, Via Celoria 16, I-20133 Milano, Italy
[4]INFN-Laboratori Nazionali del Sud, Via S. Sofia 62 Catania, Italy
[5]TNIPNE, 407 Atomistilor Street, 077125 Magurele, Romania
[6]Department of Nuclear Reactions, Institute for Nuclear Studies, ul. Hoza 69, 00-681 Warsaw, Poland
[7]Dipartimento di Fisica, Universitá di Napoli, Via Cinthia, I-80126 Napoli, Italy
[8]Dipartimento di Fisica, Universitá di Catania, Via A. Doria 64, I-95123 Catania, Italy
[9]INFN-Sezione di Padova, Via F. Marzolo 8, I-35131 Padova, Italy
[10]INFN-Laboratori Nazionali di Legnaro, Viale dellUniversitá 2, I-35020 Legnaro, Italy
[11]Rujder Bošković Institute, Bijenicka cesta 54, 10000 Zagreb, Croatia

E-mail: `domenico.torresi@lns.infn.it`

Abstract. The elastic scattering excitation function for ^{15}O on ^{4}He was measured - for the first time - by using the Inverse Kinematic Thick Target scattering method. The obtained spectrum was analysed in an R-matrix framework providing spectroscopic information for several states in the excitation energy of the nucleus ^{19}Ne from 4.8 to 9 MeV. Eight of them are newly observed states. The set-up and the experimental technique will be described in detail and the results will be shown and discussed.

1. Introduction

The first evidence of the presence of α cluster structures concerned nuclei which have even and equal numbers of protons and neutrons (so-called α-conjugate nuclei) like ^{8}Be, ^{12}C, ^{16}O. Probably one of the best examples of α cluster structure in α-conjugate nuclei is given by ^{20}Ne that is known to have a number of states associated with a well developed cluster structure comprising ^{4}He and ^{16}O closed-shell cores. It was found that these states can be grouped in several rotational bands [1, 2, 3]. Moreover the fact that these bands form inverse parity doublets offers further evidence of a mass asymmetric configuration: ^{4}He and ^{16}O. Also non-α-conjugate nuclei can manifest cluster structure, indeed, it is expected that – moving out of the valley of stability – light unstable nuclei may also exhibit cluster behaviour. Examples are ^{6}Li and ^{7}Li with pronounced α-d and α-t cluster structure in their ground state. The presence of the cluster

configurations in the ground state of these nuclei is related to their very low binding energy, close to the cluster decay threshold.

The study of unstable systems presents many difficulties, due mainly, to the low intensities typical for radioactive ion beams. Therefore, few significant experimental studies have been performed so far. Studying unstable nuclei is difficult also because often the energy spectrum of these nuclei is poorly known. This difficulty can be partially overcome by comparing the energy spectrum of the nucleus under investigation with that of the associated mirror nucleus. The study of analogue states for isobars can indeed yield important spectroscopic information.
The present work shows results of the search for cluster structure in ^{19}Ne by means of resonant scattering using a radioactive beam ^{15}O on a ^{4}He gas target.

2. Experiment

2.1. Experimental technique

The Thick Target Inverse Kinematics scattering method (TTIK) with gas targets was firstly developed in Refs. [4] and [5] for the measurement of the elastic scattering excitation function. The main advantage of the technique is that it allows the elastic scattering cross-section to be measured over a wide energy range using a single beam energy. This characteristics make the technique particularly suitable for the use with Radioactive Ion Beams (RIBs) that usually have intensities orders of magnitude lower than stable beams. The technique consists of sending a beam on a gas target (typically a scattering chamber filled with helium) with such a thickness (pressure) so as to fully stop the beam before it reaches the detectors placed at and around zero degrees in the laboratory system. The gas acts at the same time as target and as degrader of the beam energy. The interaction between projectile and target nuclei can occur at different positions along the beam trajectory, and thus at different energies. Thanks to the different stopping powers of the gas for heavy projectiles and light recoils, the recoiling particles can reach a detector placed at zero degrees in the laboratory system, while the particles of the beam are stopped before reaching the detectors. From the measurement of the recoil energy, one can deduce the interaction position along the beam direction and the energy of the scattering event. This relationship is univocal, one is sure that the detected light recoils originate from elastic scattering. Thus, the Elastic Scattering Excitation Function, (ESEF) in a given energy range, can be measured by using a single beam energy. The extent of the energy range investigated depends, of course, on the initial beam energy.

2.2. Beam production

The experiment has been performed by using a ^{15}O RIB [6] produced by the in-flight facility EXOTIC [7, 8] at the Laboratori Nazionali di Legnaro (LNL, Italy). The facility uses primary heavy ion beams delivered by the XTU tandem Van de Graaff accelerator. The primary beam is incident on a cryogenic gas target, that can be filled with hydrogen, deuterium or ^{3}He gas, then direct reactions like (p,n), (d,n) (d,p) and $(^{3}\mathrm{He},n)$ take place in the target and the reaction products are selected in flight and are finally sent to the secondary target.

For the production of the ^{15}O beam a primary $^{15}\mathrm{N}^{5+}$ beam at energy of 80 MeV impinged on a H_2 cryogenic gas target at a pressure of 1 bar and a temperature of 93 K, corresponding to an equivalent target thickness of about 1.35 mg/cm^2 of H_2. The ^{15}O beam, produced by means of the two-body reaction $p(^{15}\mathrm{N},^{15}\mathrm{O})n$ (Q_{val}=−3.54 MeV), was selected and purified from the scattered primary ^{15}N beam and other contaminant nuclei produced in the interaction between the primary beam and the H_2 target by means of a set of optical elements and collimators. Two parallel-plate avalanche counters (PPACs) [9] and a set of silicon surface barrier detector were used for different purposes: the former to optimise the beam intensity and the latter for the beam diagnostic and on-line monitoring. The two PPACs were placed downstream prior to the

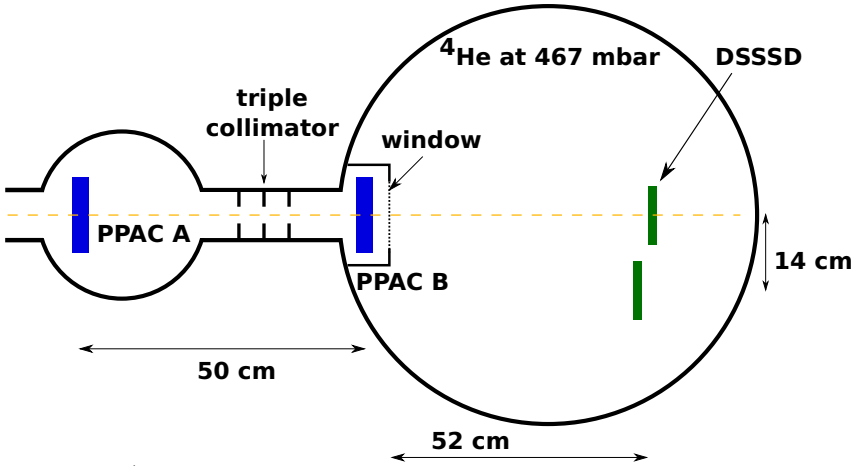

Figure 1. (color online) Schematic view of the experimental apparatus. The detection system consisted of one DSSSD and two PPACs required for beam counting and the time-of-flight measurement.

beam entering the scattering chamber for beam diagnostic purposes. The ^{15}O beam energy was 28.5 MeV and its intensity was in the range 1-2$\times10^4$ particles/s with ≈99% purity.

2.3. Experimental apparatus

The experiment was performed using the scattering chamber of the EXOTIC beam line filled with ^{4}He gas at a pressure of around 467 mbar, enough to stop the ^{15}O beam at 28.5 MeV before reaching the silicon detector. The chamber was separated from the high vacuum beam line by a 2.2 μm thick Havar window. The pressure and the temperature of the helium gas were monitored by two capacitance manometers and a thermocouple device. It was verified that the temperature did not change appreciably during the whole experiment and that the two manometers were always giving consistent pressure values within their precision. The detection of the recoiling ^{4}He relied on a 6$\times$6 cm^2 wide, 300 μm thick Double Sided Silicon Strip Detector (DSSSD) placed at zero degrees, that is part of a larger detection apparatus EXPADES [9]. Moreover two PPACs placed before the window were utilised for various purposes: first they were used for an on-line monitoring of the beam; second they provided the secondary ^{15}O beam profile by means of the event-by-event reconstruction of the trajectory; third for counting the beam particles and, finally, for timing purposes. The time-of-flight measurement between the entering of the ^{15}O particle and the following detection of a recoiling ^{4}He is used in the present experiment for the particle identification as will be shown in the next section. In Fig. 1 a sketch of the scattering chamber and the experimental apparatus is shown.

3. Data Analysis

The goal of the analysis is to deduce the elastic scattering excitation function in the centre of mass energy from the detected energy of the recoiling α particles. The first step in the analysis is to identify the recoiling α-particles and separate from other particles coming from reaction or as contaminants of the secondary beam. In Fig. 2 the plot of ToF versus detected energy is shown. The regions corresponding to α particles coming from elastic scattering and protons are easily identified. On top of the two dimensional spectrum a continuous red line is drawn that corresponds to a calculation of the ToF as a function of energy for elastically scattered α particles and a short dotted line corresponding to a calculation of the inelastic scattering to the excited states of the ^{15}O at 5.2 MeV. It can be clearly seen that the first excited state is scarcely

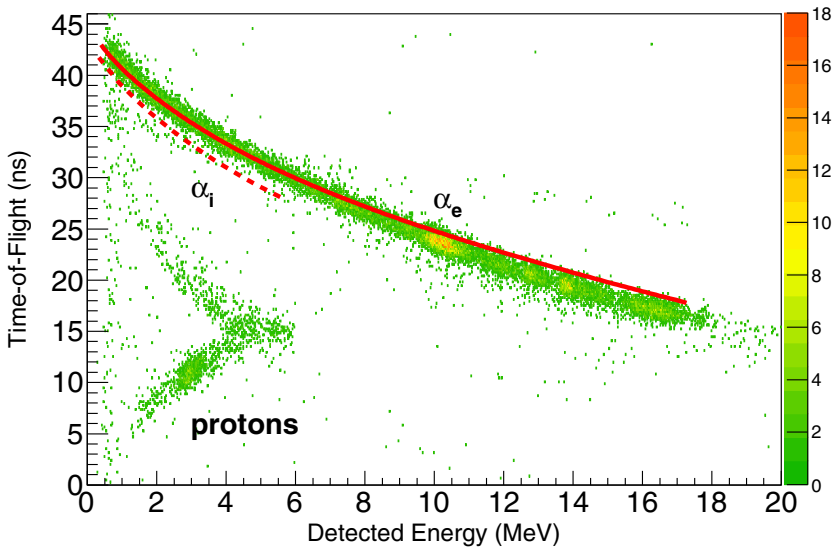

Figure 2. A plot of detected energy versus ToF. It is possible to distinguish α particles originating from an elastic scattering process and protons. The calculated distribution of α particles is indicated by the red continuous line. The red short-dashed line corresponds to α particles originating from inelastic scattering, demonstrating that events from this process have not been observed at a significant level. Adapted from Fig. 2 of Ref.[10].

populated or is not populated at all. Therefore, the ToF measurements in this case was used not only for the particle identification but also to make sure that inelastic scattering does not contaminate the elastic scattering spectrum.

Once the α particles corresponding to elastic scattering events are selected, through use of a graphical window 2D, the detected energy spectrum has to be transformed in ESEF. Indeed, the α particles are detected with an energy that is different from their energy immediately after the scattering, since they have to travel the distance between the scattering point and the detector that is filled with helium gas. The α particles lose an energy, ΔE, that is not known *a priori* since the scattering point is not known.

A calculation that associates each position at which the scattering events occurred to a corresponding energy of the α particles at the detector has been performed. This calculation requires as input, the geometry of the detection apparatus, the pressure and temperature of the gas and the stopping power of ^{4}He gas for ^{15}O and α particles. From this it follows that the knowledge of the stopping power is of fundamental importance to obtain a reliable elastic scattering excitation function. Indeed, the effect of using the wrong stopping powers does not simply shift the spectrum but deforms it, this has been demonstrated by Zadro *et al.* [11] where the elastic scattering of ^{9}Be on ^{4}He was measured and compared to the ESEF obtained using the stopping power of ^{4}He for ^{9}Be calculated by SRIM [12]. The importance of knowing the stopping power to high accuracy, for the current experiment is further illustrated by Fig. 3 where the same detected energy spectrum was transformed in ESEF using two different stopping power functions calculated using codes SRIM [12] and dedx [13]. The two different stopping power curves are shown in Fig. 4.

Due to the strong influence of the stopping power on the final ESEF, the stopping power for oxygen in helium gas was measured in a separate experiment [14], and the final ESEF, shown in Fig. 5 was obtained using this experimentally measured stopping power.

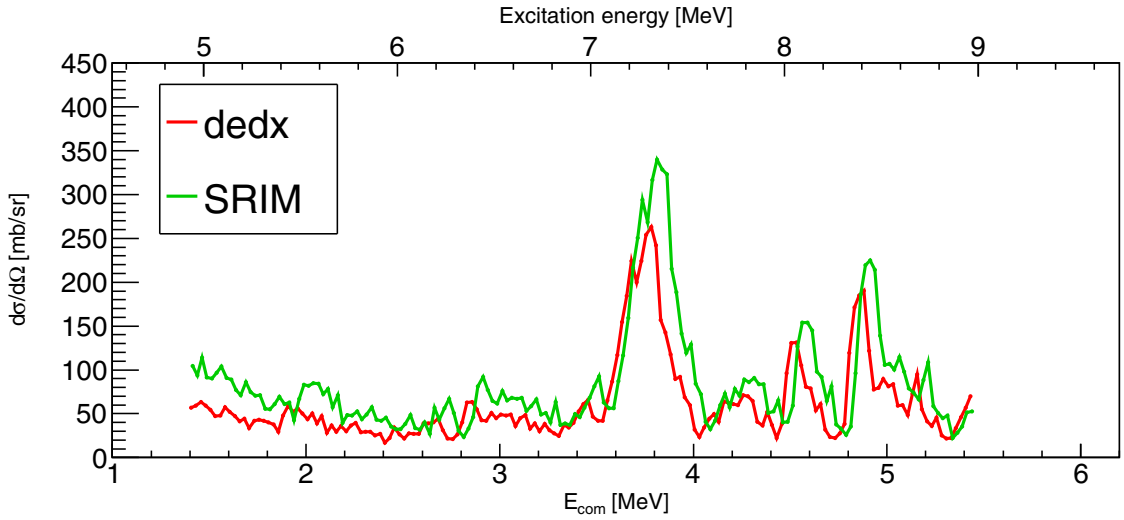

Figure 3. Elastic scattering excitation function deduced using two different stopping power functions calculated by the code SRIM (black curve) and the code *dedx* (green curve).

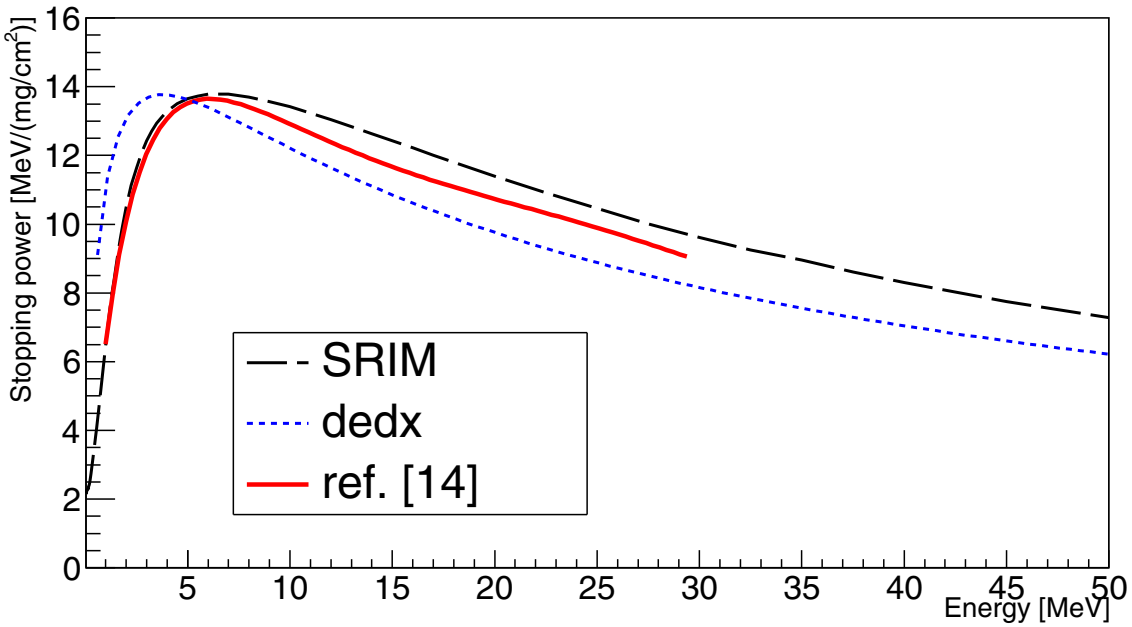

Figure 4. The stopping power curves for ^{16}O in ^{4}He gas. The stopping power calculated by the code SRIM (black dashed line) and by the code *dedx* (dotted blu line) is compared with the experimentally measured one (red continuous line.

4. R-matrix calculation

In order to determine the main properties of the observed resonances: widths, partial decay branches, energies and spins, an R-matrix calculation was performed. A comprehensive description of the R-matrix theory can be found in Ref. [15]. A full R-Matrix fit was performed using Azure2 [16]. The spins and energies of states from the mirror nucleus, ^{19}F [17], were used as a starting point for the fit; a powerful technique, with a good agreement between the energy levels in each nucleus. A two channel calculation was performed to fit the data: ^{15}O+α and ^{18}F+p. Levels in the 5.3-8.9 MeV excitation-energy region have been investigated, with a number of newly observed states in this work. Furthermore, partial widths have been extracted for the observed levels, for many of them it is the first time measure-width data has been available.

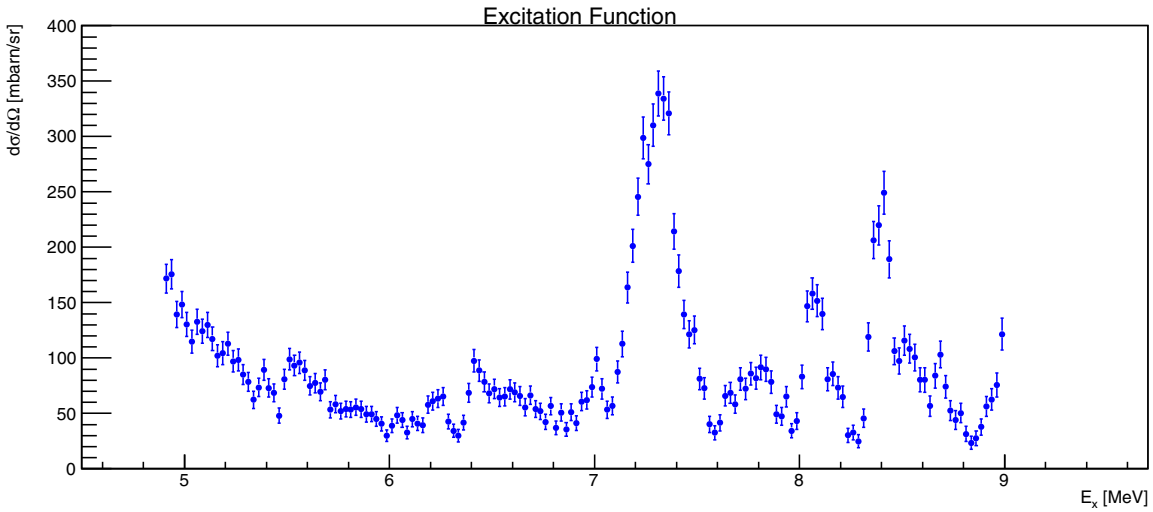

Figure 5. Elastic scattering excitation function deduced using the experimentally measured stopping power.

The results of R-matrix calculation will be discussed in details in a Ref. [10].

5. Conclusion

We have reported the measurements of the ^{15}O-α elastic scattering excitation function by using the TTIK method. The technique included a time-of-flight measurement that allows the discrimination of elastic scattering from other reaction mechanisms. The stopping power of the helium gas for the oxygen isotope was measured to avoid systematic errors that the use of a calculated stopping power can introduce in the deduction of the centre-of-mass energy from the detected energy. The excitation function was measured for excitation energies in the range of 5.3 to 8.9 MeV and it was analysed using an R-matrix approach. The R-matrix calculation, that reproduces rather well the experimental data, includes several new resonances with evidence for pronounced cluster structure [10].

Acknowledgements

The present work has received funding from the European Unions Horizon 2020 research and innovation programme under the Marie Sklodowska-Curie grant agreement No 659744. The UK STFC is acknowledged for providing funding under grant ST/L005751/1. M.Z. was partially supported by the Croatian Science Foundation under Project No. 7194.

References

[1] T. Tomoda and A. Arima, Nucl. Phys. A **303**, 217 (1978).
[2] S.R. Riedhauser *et al.*, Phys. Rev. C **29** (1984) 1961.
[3] H.T. Richards, Phys. Rev. C **29**, 276 (1984).
[4] K.P. Artemov *et al.*, Sov. J. Nucl. Phys. **52**, 634 (1990).
[5] K. Kallman *et al.*, Nucl. Instr. And Meth. in Phys. Res., A **338**, 413 (1994).
[6] D. Torresi, C. Wheldon *et al.*, LNL Annual Report (2014) p19, see *http://www.lnl.infn.it/∼annrep/read_ar/2014/ contributions/pdfs/019_A_61_A056.pdf.*
[7] V.Z. Maidikov *et al.*, Nucl. Phys. A **746**, 389c (2004).
[8] M. Mazzocco *et al.*, Nucl. Instr. and Meth. in Phys. Res. B **317**, 223 (2013).
[9] D. Pierroutsakou *et al.*, Nucl. Instr. and Meth. in Phys. Res. A **834**, 46 (2016).
[10] D. Torresi *et al.*, Phys. Lett. B. submitted.
[11] M. Zadro *et al.*, Nucl. Instr. and Meth. in Phys. Res. B **259**, 836 (2007).
[12] J.F. Ziegler, Nucl. Instr. and Meth. in Phys. Res. B **219-220**, 1027 (2004).

[13] Computer Program DEDX (University of Birmingham, UK) unpublished. Based on computer program SPAR, T.W. Armstrong, K.C. Chandler, ORNL-4869 (Oak Ridge National Laboratory, US) 1973 and T.W. Armstrong, K.C. Chandler, Nuclear Instruments and Methods **113**, 313 (1973).
[14] D. Torresi *et al.*, Nucl. Instr. and Meth. in Phys. Res. B **389-390**, 1 (2016).
[15] A,M. Lane and R.G. Thomas, Reviews of Modern Physics **30**, 257 (1958).
[16] R. Azuma *et al.*, Phys. Rev. C **81**, 045805 (2010).
[17] D.R. Tilley, H.R. Weller, C.M. Cheves and R.M. Chasteler, Nucl. Phys A **595**, 1 (1995).